

Positive and negative ion mode ESI-MS and MS/MS for studying drug–DNA complexes

Frédéric Rosu, Sophie Pirote, Edwin De Pauw, Valérie Gabelica*

Laboratoire de Spectrométrie de Masse, Université de Liège, Institut de Chimie, Bat. B6c, B-4000 Liège, Belgium

Received 17 August 2005; received in revised form 29 November 2005; accepted 30 November 2005

Available online 9 January 2006

Abstract

We report systematic investigation of duplex DNA complexes with minor groove binders (Hoechst 33258 and 33342, netropsin and DAPI) and intercalators (daunomycin, doxorubicin, actinomycin D, ethidium, cryptolepine, neocryptolepine, *m*-Amsacrine, proflavine, ellipticine and mitoxantrone) by ESI-MS and ESI-MS/MS in the negative ion mode and in the positive ion mode. The apparent solution phase equilibrium binding constants can be determined by measuring relative intensities in the ESI-MS spectrum. While negative ion mode gives reliable results, positive ion mode gives a systematic underestimation of the binding constants and even a complete suppression of the complexes for intercalators lacking functional groups capable of interacting in the grooves. In the second part of the paper we systematically compare MS/MS fragmentation channels and breakdown curves in the positive and the negative modes, and discuss the possible uses and caveats of MS/MS in drug–DNA complexes. In the negative mode, the drugs can be separated in three groups: (1) those that leave the complex with no net charge; (2) those that leave the complex with a negative charge; and (3) those that remain attached on the strands upon dissociation of the duplex due to their positive charge. In the positive ion mode, all complexes fragment via the loss of protonated drug. Information on the stabilization of the complex by drug–DNA noncovalent interactions can be obtained straightforwardly only in the case of neutral drug loss. In all other cases, proton affinity (in the positive ion mode), gas-phase basicity (in the negative ion mode) and coulombic repulsion are the major factors influencing the fragmentation channel and the dissociation kinetics.

© 2005 Elsevier B.V. All rights reserved.

Keywords: Drug–DNA complexes; ESI-MS; MS/MS; Negative ion mode; Gas-phase basicity

1. Introduction

Since intact noncovalent complexes have been observed for the first time by electrospray mass spectrometry [1], the interest in the field has constantly been growing, and ESI-MS has now analytical applications for the study of noncovalent complexes, notably for the determination of the complex stoichiometries, and for the evaluation of equilibrium binding constants. Still, even 15 years later, the investigation of a new family of complexes requires preliminary tests to assess whether the apparent binding constants are reliable [2,3]. An even more exploratory subject concerns the information that can be obtained on the complexes using all the possible MS/MS techniques [4]. Gas-phase dissociation approaches are extremely attractive because it is the only experimental approach that allows probing the

purely intermolecular interactions in the absence of solvent [5].

Our group is particularly interested in the research field of drug–DNA interactions. Parsing the binding free energies in those complexes has also been attempted [6–10]. For drug–DNA interactions, Chaires has proposed a conceptual model that assumes that the observed binding free energy $\Delta G^{\circ}_{\text{obs}}$ results from the additive contributions of five terms [8]: $\Delta G^{\circ}_{\text{conf}}$ (contribution from conformational changes upon complex formation), $\Delta G^{\circ}_{\text{tr}}$ (losses in translational and rotational degrees of freedom), $\Delta G^{\circ}_{\text{hyd}}$ (hydrophobic transfer of drug from the solution into its DNA binding site), $\Delta G^{\circ}_{\text{pe}}$ (polyelectrolyte contribution), and $\Delta G^{\circ}_{\text{mol}}$ (contribution from the formation of noncovalent molecular interactions between the drug and the DNA). These molecular interactions include hydrogen bond formation, van der Waals interactions and electrostatic interactions. Those different terms can all be quantified or determined experimentally except $\Delta G^{\circ}_{\text{mol}}$. It is only possible to estimate the $\Delta G^{\circ}_{\text{mol}}$ contribution due to modification of functional

* Corresponding author.

E-mail address: v.gabelica@ulg.ac.be (V. Gabelica).

groups by performing accurate binding studies and structural studies but this is extremely labor intensive. We therefore try to assess whether MS/MS could help getting experimental data on $\Delta G^\circ_{\text{mol}}$.

In order to assess the validity of mass spectrometric techniques for DNA–ligand complexes, we used 12-mer duplex DNA, and a panel of ligands having well-known binding modes. Small molecule interaction with duplex DNA can proceed basically via two mechanisms: intercalation and minor groove binding. The two grooves of DNA differ in size and in topology: the major groove is wider and is generally the recognition region for proteins. The minor groove is narrower and surrounded by the sugar-phosphate-sugar chains. Minor groove binders are synthetic molecules that interact with B-DNA in the minor groove. They have a crescent shape and fit in the minor groove without distorting the double helix. Hydrogen bond donor groups at the inner edge make H-bonds with the base pairs of each strand. The drugs we studied here all have a preference for AT-rich regions of DNA for three reasons: (i) the $-\text{NH}_2$ group on guanine causes steric hindrance in the groove; (ii) the minor groove is narrower in AT-rich regions, which is favorable to van der Waals contacts with the sugars; and (iii) the AT regions have a more negative electrostatic potential, which is favorable for the binding of positively charged molecules [11,12]. Minor groove binders can form either 1:1 or 2:1 complexes in a given AT rich site. Intercalators bind to DNA by insertion of their planar aromatic chromophore between DNA base pairs [13,14]. Simple intercalators have few substituents, but others like actinomycin D and doxorubicin are more complex, and substituents can interact with the minor or the major groove and participate to a wide variety of molecular interactions. A conceptual model for intercalation has been proposed [8]. First, DNA must undergo conformational transition (the double helix is unwound) to form the intercalation site. Second, the transfer of the intercalator from the solution to the intercalation site is hydrophobic. Finally, a variety of noncovalent molecular interactions can be formed (stacking of the aromatic rings, hydrogen bonding, van der Waals contacts, . . .). These intermolecular interactions are those we would like to probe using MS/MS approaches.

Most ESI-MS investigations of DNA and drug–DNA complexes have been carried out using negative ion mode. This follows logically from the knowledge that the phosphodiester backbone of the DNA has a $pK_a < 1$, and is therefore fully deprotonated under most experimental conditions. Several papers demonstrated that this approach gives reliable apparent binding constants in the case of duplex DNA [15,16], quadruplex DNA [17], and different RNA structures [18,19]. Some papers were recently published on ESI mass spectra of DNA acquired using positive ion mode [20,21]. We therefore wanted to assess whether the positive ion spectra are likely to provide an accurate picture of the drug–DNA complexes present in solution. Comparisons between positive and negative ion modes are reported here. The second part of the paper is devoted to a systematic investigation of MS/MS on DNA–drug complexes, in positive and negative ion modes, in order to address the whys and wherefores of tandem mass spectrometry in these systems. Only a few papers on MS/MS of drug–DNA complexes have been published

to date [22–26], our goal was to rationalize these observations in the light of a systematic study complexes of well-known structures.

2. Experimental

2.1. Materials

The duplexes Dk33 (d(CGTAATTACG)₂), Dk66 (d(CGCGAATTCGCG)₂) and Dk100 (d(CGCGGGCCCGCG)₂) were prepared by heating 100 μM single strand in 100 mM aqueous NH_4OAc to yield a 50 μM stock solution at neutral pH. The single strands were purchased from Eurogentec (Angleur, Belgium) and used without further purification. The drug stock solutions were 100 or 200 μM in water or methanol for the non-water soluble ones. For ESI-MS, drug–duplex equimolar mixtures (2, 4 and 10 μM) were prepared in 100 mM NH_4OAc and 20% methanol. The concentrations of the stock solutions were remeasured no more than 3 days before the ESI-MS experiments. For ESI-MS/MS, relative concentrations are not critical. Usually 10 μM equimolar solutions were used, but a two-fold excess of drug was used for the weak binders to have more signal for the parent ion. All ligands were purchased from Sigma–Aldrich (www.sigma-aldrich.com), except cryptolepine and neocryptolepine [27] which were donated by Luc Pieters (University of Antwerp, Belgium). Cryptolepine, neocryptolepine, ellipticine and *m*-Amsacrine were solubilized in methanol, and all other ligands are solubilized in bi-distilled water.

2.2. Mass spectrometry

Two papers describing the influence of the collision regime on the dissociation of duplex DNA alone have been published [28,29]. Briefly, collision-induced dissociation (CID) of duplex DNA in the quadrupole collision cell of a QTOF2 instrument produces the single strands which share the available charges of the duplex. Upon CID in the QTOF2, the main fragmentation pathway remains the noncovalent dissociation into single strands at high collision energies, but the loss of neutral base (G, A, C) becomes more and more abundant as the hexapole collision voltage is lowered. It was therefore concluded that high collision energies had to be preferred in order to observe predominantly the noncovalent dissociation channels. In order to probe the drug–DNA interaction energy via the MS/MS, we should observe ideally the noncovalent dissociation of the drug from the duplex. Therefore, we used the QTOF instrument for all MS/MS experiments on drug–DNA complexes presented in this study.

All experiments were performed on a Q-TOF Ultima Global (Micromass, now Waters, Manchester, UK) with the normal ESI source. In negative ion mode the capillary voltage was set to -2.2 kV and the cone voltage to 35 V. The RF lens 1 voltage was set to 25 V for Dk33 and complexes, and to 35 V for Dk66 and Dk100 and complexes. In positive ion mode ESI-MS, the capillary voltage was set to 3.0 kV, the cone voltage to 100 V, and the RF lens 1 voltage to 100 V. In both modes, a hexapole collision voltage of 10 V was used for full scan MS. This collision voltage is proportional to the internal energy or the center

of mass kinetic energy of the ions. In MS/MS, the parent ion of interest was selected in the first quadrupole, and the hexapole collision voltage was varied. In both modes, the argon pressure in the collision hexapole (3.0×10^{-5} mbar \pm 5%) and the source pressure (2.70 mbar) were carefully kept constant. Source block and desolvation temperatures were set to 70 and 100 °C, respectively.

2.3. AM1 semi-empirical calculations

All proton affinity calculations were performed at the AM1 level using Spartan'04 for Windows. All plausible protonation sites were tried (see text), and complete conformational search was performed for the neutral and each protonated form. The molecule PA is defined in Eq. (1):

$$\text{PA} = \Delta H^\circ_f(\text{molecule}) + \Delta H^\circ_f(\text{H}^+) - \Delta H^\circ_f(\text{molecule} + \text{H}^+) \quad (1)$$

The ΔH°_f (molecule) and ΔH°_f (molecule + H⁺) are calculated by AM1, and ΔH°_f (H⁺) value used is 365.7 kcal/mol [30].

3. Results and discussion

3.1. Full scan ESI-MS

3.1.1. Minor groove binders

We have studied the complexes formed between the minor groove binders represented in Fig. 1 and the three duplexes d(CGTA₃T₃TCG)₂ (Dk33), (CGCGAATTCGCG)₂ (Dk66) and (CGCG₃C₃GCG)₂ (Dk100). The number in DkXX indicates the percentage of GC base pairs. In a previous paper, where we compared the values of the equilibrium binding constants obtained by ESI-MS (negative mode) and those determined by fluorescence titrations, we have shown that ESI-MS relative intensities were indeed reflecting the solution binding constants [16]. We used the same procedure here for calculating the equilibrium binding

constants. The values determined by ESI-MS in the negative ion mode are given in Table 1. The binding constants K_1 and K_2 are defined as:

$$K_1 = \frac{[C_{1:1}]}{[\text{DNA}][\text{drug}]} \quad (2)$$

$$K_2 = \frac{[C_{2:1}]}{[C_{1:1}][\text{drug}]} \quad (3)$$

The values obtained previously for duplex Dk66 [16] (in reference [16], Dk66 was noted DK) using a Finnigan LCQ are in excellent agreement with the values obtained here on the Micromass Q-TOF Ultima. The amount of bound minor groove binder molecule increases when the percentage of AT base pairs increases. The minor groove binders studied show no interaction with a duplex containing 100% GC base pair d(CGCG₃C₃GCG)₂ (Dk100). These results are consistent with the known AT base pair preference of minor groove binders, and demonstrate the absence of false positives in negative ion mode ESI-MS.

We then compared the positive and negative ion mode ESI-MS. Fig. 2 shows the negative ion mode (top) and positive ion mode (bottom) spectra obtained for an equimolar mixture ($C_0 = 5 \mu\text{M}$) of the duplex d(CGCGAATTCGCG)₂ (Dk66) and the minor groove binder Hoechst 33258. Only the 5⁻ or 5⁺ charge state is shown for clarity of the figure. The stoichiometry of the complexes observed is identical for the two ion modes (only 1:1 complex), but the relative intensity of Duplex-Hoechst 33258 complex is much lower in positive ion mode. Table 2 shows the values of the determined association constants at three different concentrations for the minor groove binders and the three duplexes with different percentage of GC base pairs. Again, for the duplex Dk100, no complex is detected, indicating that no false positives are obtained in positive ion mode either. For Dk33 and Dk66, 1:1 complexes between the duplex and the minor groove binders are observed, but binding constants are much lower than those determined in negative mode (Table 1).

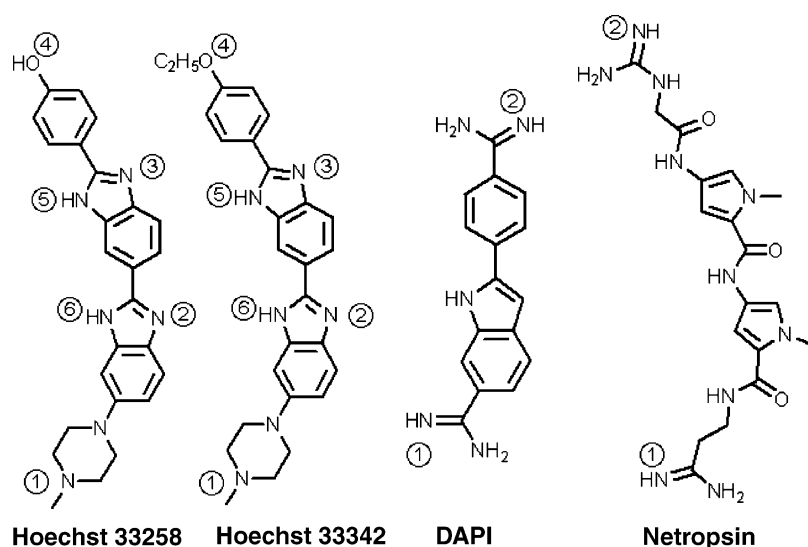


Fig. 1. Structure of the minor groove binders, drawn in their neutral form. In water at physiological pH, Hoechst 33258 and 33342 are singly protonated (site ①), and DAPI and netropsin are doubly protonated (sites ① and ②).

Table 1

Results of the negative ESI-Q-TOFMS determined equilibrium association constants at three different concentrations for the minor groove drugs (Hoechst 33258 and 33342, DAPI, netropsin) and the duplex d(CGTA₃T₃TCG)₂ (Dk33), the duplex (CGCGAATTCGCG)₂ (Dk66) and the duplex (CGCG₃C₃GCG)₂ (Dk100)

Duplex	C ₀ (μM)	Hoechst 33258		Hoechst 33342		DAPI		Netropsin	
		K ₁ (M ⁻¹)	K ₂ (M ⁻¹)	K ₁ (M ⁻¹)	K ₂ (M ⁻¹)	K ₁ (M ⁻¹)	K ₂ (M ⁻¹)	K ₁ (M ⁻¹)	K ₂ (M ⁻¹)
Dk33	2	5.1 × 10 ⁷	ND	4.7 × 10 ⁷	ND	8.9 × 10 ⁶	ND	7.5 × 10 ⁶	ND
	4	4.8 × 10 ⁷	ND	2.5 × 10 ⁷	ND	8.0 × 10 ⁶	ND	4.3 × 10 ⁶	ND
	10	3.2 × 10 ⁶	ND	1.6 × 10 ⁷	ND	6.1 × 10 ⁶	ND	1.8 × 10 ⁶	ND
		4.3 × 10⁷		2.9 × 10⁷		7.6 × 10⁶		4.3 × 10⁶	
Dk66	2	1.0 × 10 ⁷	ND	3.0 × 10 ⁷	ND	3.0 × 10 ⁶	ND	4.7 × 10 ⁶	ND
	4	1.2 × 10 ⁷	ND	0.7 × 10 ⁷	ND	2.1 × 10 ⁶	ND	2.2 × 10 ⁶	ND
	10	2.4 × 10 ⁷	ND	0.5 × 10 ⁷	ND	8.5 × 10 ⁶	ND	1.4 × 10 ⁵	ND
		1.5 × 10⁷		1.4 × 10⁷		2.0 × 10⁶		2.8 × 10⁶	
Dk100	2	ND	ND	ND	ND	ND	ND	ND	ND
	4	ND	ND	ND	ND	ND	ND	ND	ND
	10	ND	ND	ND	ND	ND	ND	ND	ND

The mean values of the measurements at three concentrations are indicated in bold. ND, not detected (signal to noise ratio < 3).

3.1.2. Intercalators

The intercalators studied here (Fig. 3) have DNA binding site sizes of two base pairs (ethidium, *m*-Amsacrine, proflavine, mitoxantrone, cryptolepine and neocryptolepine), three base pairs (daunomycin and doxorubicin), or 4–5 base pairs (actinomycin D). The charge and the polarity of these drugs are quite different. Cryptolepine, neocryptolepine, ellipticine and *m*-Amsacrine are neutral non-polar intercalators; mitoxantrone, proflavine, daunomycin, doxorubicin and actinomycin D are protonated at neutral pH, and ethidium is a quaternary ammonium. According to their behavior in positive ion mode ESI-MS, the intercalators can be separated in two classes.

The first class of intercalators contains the compounds having some functional group interacting in the minor groove of the double helical DNA (actinomycin D, daunomycin, and doxorubicin). For these ligands, a complex is observed in positive

ESI-MS. Fig. 4 shows the spectra obtained in negative and positive mode with equimolar solutions (5 μM) of daunomycin or doxorubicin and the duplex Dk66 (d(CGCGAATTCGCG)₂). In the negative ion mode, 1:1 (one drug-one duplex) and 2:1 (two drugs-one duplex) complexes are observed for both ligands. The values of the equilibrium association constants obtained by negative ESI-MS are in good agreement with the literature (K₁ = 6.2 × 10⁵ M⁻¹ for daunomycin binding to calf thymus DNA in 0.185 M NaCl [31]). The amount of drug bound to the double helix is higher with doxorubicin. The reason is that doxorubicin has a supplementary hydroxyl group that can form a hydrogen bond with the DNA duplex. This result totally agrees with published data obtained by isothermal titration calorimetric experiments on these two ligands [7,32]. The results obtained in positive ion mode are similar as with the minor groove binder: the same stoichiometries are observed, but the intensities of the peaks corresponding to the complex are lower in comparison with the negative ion mode. The same behavior is observed with actinomycin D.

The second class of intercalators comprises molecules that interact only via intercalation (stacking) between the base pairs. These intercalators include cryptolepine, neocryptolepine, *m*-Amsacrine, ethidium, proflavine, mitoxantrone and ellipticine. For all these ligands, no complex could be observed in the positive ion mode whatever the sequence of the double-stranded DNA used. This is in total contradiction with both the ESI-MS negative ion mode results and also all the published literature data where it has been demonstrated that all of these drugs bind to DNA. Fig. 5 shows mass spectra obtained in negative ion mode (top) and positive ion mode (bottom) with ethidium and the DK66 duplex.

3.1.3. Discussion

There are two obvious problems in studying drug–DNA complexes in positive ion mode: (1) complexes cannot be detected for ligands interacting only by intercalation (stacking interactions with the DNA bases); and (2) for the other drugs where a complex is observed, its relative intensity is too low compared to its relative abundance in the solution, and this leads to a dramatic

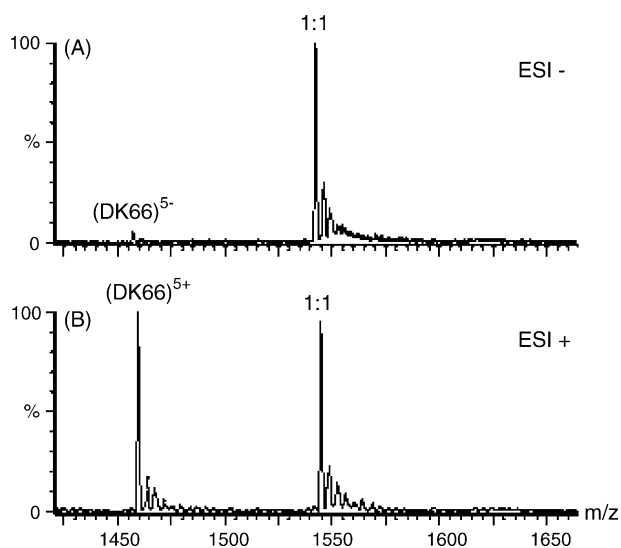


Fig. 2. ESI-MS full scan spectra of equimolar mixtures (C₀ = 5 μM) of Hoechst 33258 with the duplex d(CGCGAATTCGCG)₂ (Dk66) obtained in negative ion mode (A) and positive ion mode (B). Spectra were recorded in 100 mM ammonium acetate. The small adduct peaks are sodium adducts.

Table 2
Results of the positive ion mode ESI-Q-TOFMS determined equilibrium association constants at three different concentrations for the minor groove drugs (Hoechst 33258 and 33342, DAPI, netropsin) and the duplex d(CGTA₃T₃TCG)₂ (Dk33), the duplex (CGCGAATTCGCG)₂ (Dk66) and the duplex (CGCG₃C₃GCG)₂ (Dk100)

Duplex	C ₀ (μM)	Hoechst 33258		Hoechst 33342		DAPI		Netropsin	
		K ₁ (M ⁻¹)	K ₂ (M ⁻¹)	K ₁ (M ⁻¹)	K ₂ (M ⁻¹)	K ₁ (M ⁻¹)	K ₂ (M ⁻¹)	K ₁ (M ⁻¹)	K ₂ (M ⁻¹)
Dk33	2	5.0 × 10 ⁵	ND	6.1 × 10 ⁵	ND	7.8 × 10 ⁵	ND	3.8 × 10 ⁶	ND
	4	3.9 × 10 ⁵	ND	3.5 × 10 ⁵	ND	3.6 × 10 ⁵	ND	1.9 × 10 ⁶	ND
	10	1.9 × 10 ⁵	ND	1.6 × 10 ⁵	ND	1.2 × 10 ⁵	ND	0.9 × 10 ⁶	ND
		4.6 × 10⁵		3.7 × 10⁵		4.2 × 10⁵		2.2 × 10⁶	
Dk66	2	6.0 × 10 ⁵	ND	3.8 × 10 ⁵	ND	4.0 × 10 ⁵	ND	3.7 × 10 ⁶	ND
	4	3.6 × 10 ⁵	ND	3.0 × 10 ⁵	ND	2.3 × 10 ⁵	ND	2.5 × 10 ⁶	ND
	10	1.6 × 10 ⁵	ND	1.2 × 10 ⁵	ND	2.110 ⁵	ND	2.0 × 10 ⁵	ND
		3.7 × 10⁵		2.6 × 10⁵		2.8 × 10⁵		2.7 × 10⁶	
Dk100	2	ND	ND	ND	ND	ND	ND	ND	ND
	4	ND	ND	ND	ND	ND	ND	ND	ND
	10	ND	ND	ND	ND	ND	ND	ND	ND

The mean values of the measurements at three concentrations are indicated in bold. ND, not detected (signal to noise ratio < 3).

underestimation of the binding constant. What is therefore the problem with positive ion mode?

The major difference between positive and negative ion electrospray is the mechanism of charging of DNA. In negative ion mode electrospray (Fig. 6, top), the droplets carry excess negative charges consisting of DNA polyanions (10⁻⁵ M) and acetate anions (0.1 M). As a good DNA signal is obtained in the negative mode even with acetate-to-DNA ratios as large as 100,000, this suggests that DNA polyanions have a higher affinity than acetate for the droplet surface, according to the equilibrium par-

tititioning model [33,34]. In order to end up in the gas phase with only four, five or six negative charges (as usually observed for 12-mer duplexes in 0.1 M NH₄OAc), the other phosphate groups need to be neutralized by some ammonium cations, which are subsequently removed by gentle collisions. A loss of NH₃ leaves a protonated (neutral) phosphate. In the case of the DNA–drug complexes, the fact that the relative intensities in the negative ion mode reflect the relative abundances in solution indicates that there is neither non-specific aggregation, nor dissociation of the complex during electrospray.

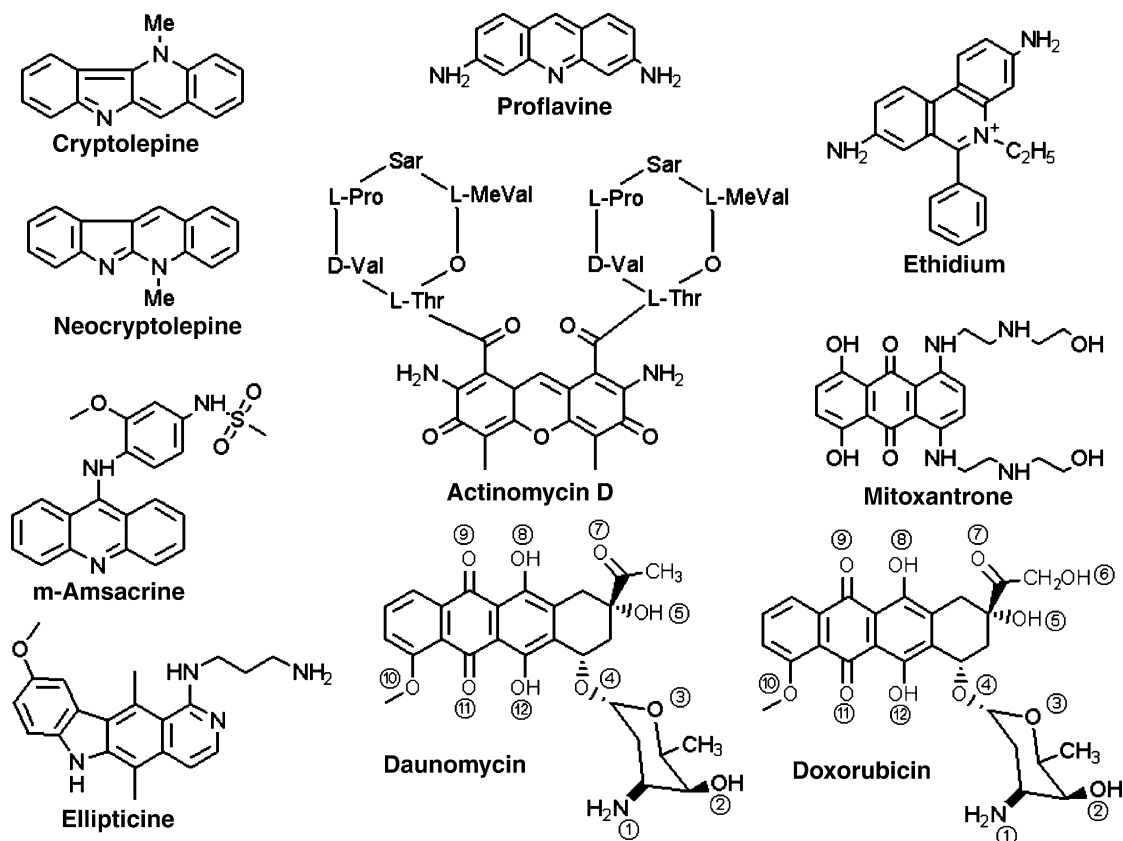


Fig. 3. Structures of the intercalators.

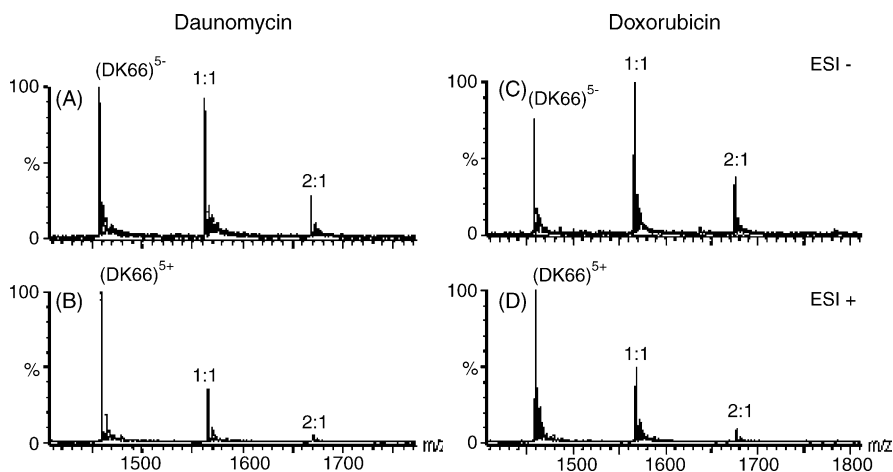


Fig. 4. ESI-MS full scan spectra of the duplex $d(\text{CGCGAATTCGCG})_2$ (Dk66) with (A) daunomycin obtained in negative ion mode; (B) daunomycin obtained in positive ion mode; (C) doxorubicin obtained in negative ion mode; (D) doxorubicin obtained in positive ion mode. Spectra were recorded in 100 mM ammonium acetate with equimolar mixtures ($C_0 = 5 \mu\text{M}$) of drug and the oligonucleotide. The small adduct peaks are sodium adducts.

In positive ion mode (Fig. 6, bottom), the surface excess charges are ammonium cations. In order to observe protonated DNA, not only must all phosphates be neutralized, but four to six protons must also be added. These extra positive charges on DNA are thought to reside on the nucleobases [35]. Whatever the ion formation mechanism (ion evaporation or formation of a charged residue), the DNA polyanions must come in close proximity to the positively charged surface containing ammonium cations. Then the ammonium cations neutralize the phosphates and protonate some bases in the major and the minor grooves. In the case of the DNA–drug complexes in positive mode, the electrospray process obviously disturbs the complex. The observation that with daunomycin and doxorubicin the relative intensities in positive mode are still proportional to binding constants is in favor a displacement of the equilibrium. However, the extent of equilibrium shifting does not depend on the

equilibrium constant, but on the DNA binding mode: ethidium has a similar binding constant as daunomycin, but is completely displaced while daunomycin complex is still detected. The difference comes from the fact that daunomycin can be retained only by some remaining H-bonds with the DNA bases in the grooves. Equilibrium shifting could come from a dramatic distortion of the DNA structure upon phosphate neutralization and further protonation on the bases. MS/MS experiments on duplex DNA in the positive ion mode address the problem of the conservation of hydrogen bonding and stacking interactions in protonated DNA ions.

3.2. MS/MS on duplex DNA in positive ion mode

The MS/MS on the oligonucleotides Dk33, Dk66 and Dk100 has been described previously [28]. Briefly, in the Q-TOF2 instrument Dk33 and Dk66 fragment via the separation of the single strands, with minor neutral base loss. Dk66 needs a higher hexapole collision voltage to fragment than Dk33, reflecting the hydrogen bond content (i.e., GC base pair content) of the duplex. Dk100 needs a higher collision voltage than Dk66 to fragment, but numerous fragmentations of the single strands themselves are observed at these high collision voltages. Here we performed MS/MS experiments in the positive ion mode in order to assess whether the hydrogen bonding and base stacking interactions are still conserved in the protonated, positively charged DNA.

In positive ion mode, the double-stranded oligonucleotides dissociate via three major channels (Eq. (4)): (i) separation into single strands; and (ii) loss of protonated base. The single strands are also observed with a base lost. At higher energy (typically >20 V collision voltage), numerous fragments coming from the breaking of covalent bonds of the single strands appear (iii).

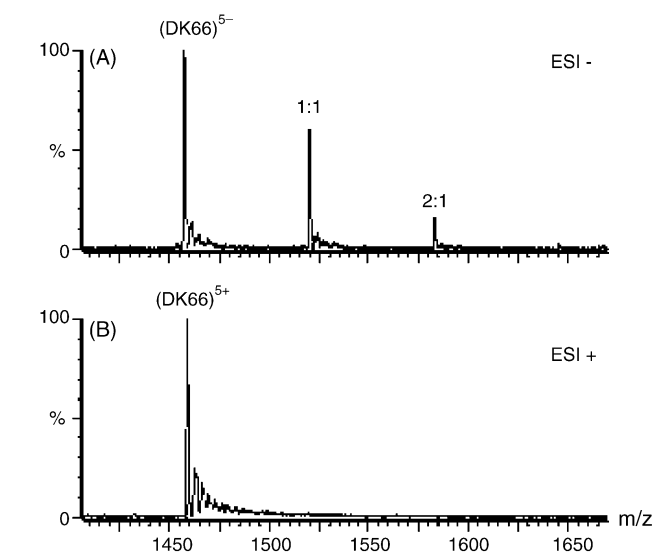
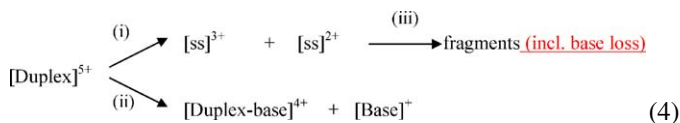


Fig. 5. ESI-MS full scan spectra of equimolar mixtures ($C_0 = 5 \mu\text{M}$) of ethidium with the duplex $d(\text{CGCGAATTCGCG})_2$ (Dk66) obtained in negative (top) and positive (bottom) ion modes. The small adduct peaks are sodium adducts.

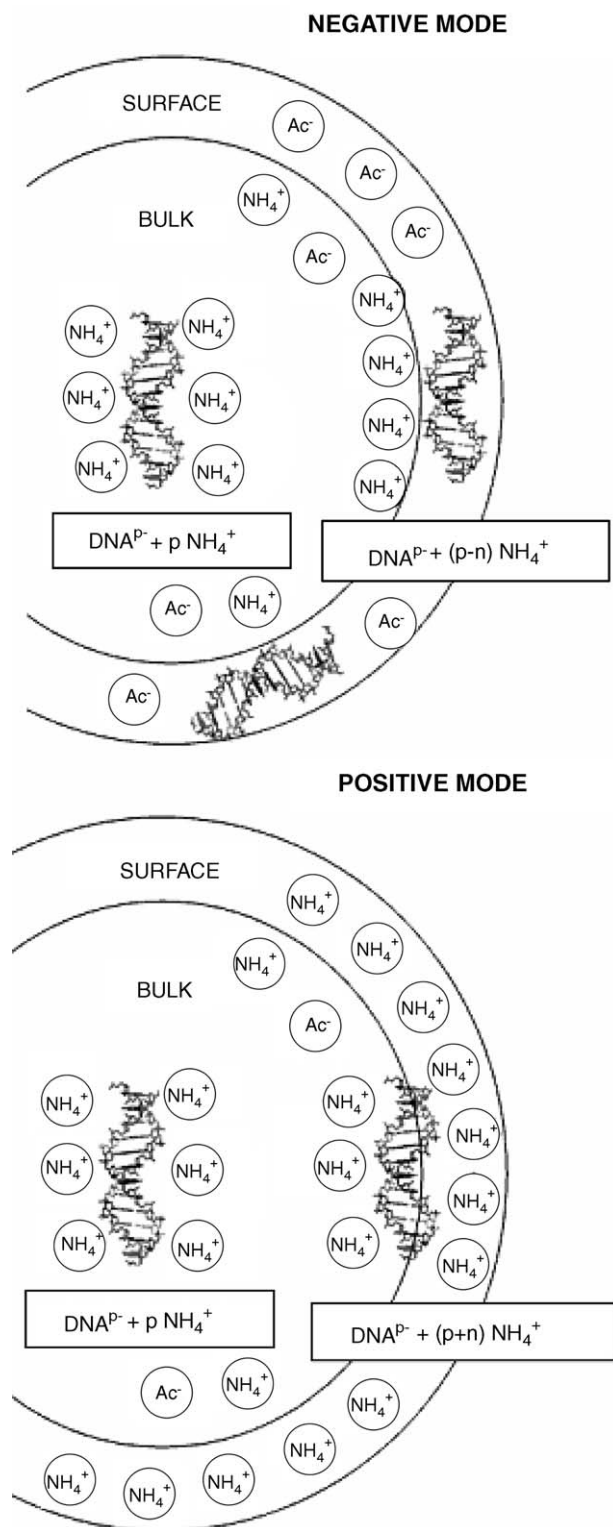


Fig. 6. Schematic representation of the droplet charging processes for a DNA solution in ammonium acetate electrolyte in negative ion mode (top) and positive ion mode (bottom).

The percentage of intact duplex is calculated using Eq. (5a), where $I(\text{base}^+)$ stands for the intensities of the peak of the protonated bases (G, A and C), $I(\text{ss}^{n+})$ stands for the sum of intensities of $[\text{ss}]^{n+}$, $[\text{ss-G}]^{n+}$, $[\text{ss-A}]^{n+}$ and $[\text{ss-C}]^{n+}$.

$$\% \text{ Intact duplex} = \frac{I(\text{duplex}^{5+}) \times 100\%}{\{I(\text{duplex}^{5+}) + I(\text{ss}^{3+}) + I(\text{ss}^{2+}) + I([\text{duplex} - \text{base}]^{4+}) + I(\text{base}^+)\}/2} \quad (5a)$$

The percentage of intact duplex as a function of the collision voltage is shown in Fig. 7(a). The duplexes with higher GC content (Dk66 and Dk100) dissociate at much higher energy than Dk33. However, the relative contribution of fragmentation pathways (i) and (ii) is duplex-dependent: the contribution of path (i) is $77 \pm 1\%$ for $[\text{Dk33}]^{5+}$, $21 \pm 3\%$ for $[\text{Dk66}]^{5+}$, and $8.3 \pm 2.5\%$ for $[\text{Dk100}]^{5+}$. We therefore calculated a breakdown curve relative to path (i) only, using Eq. (5b) for the calculation

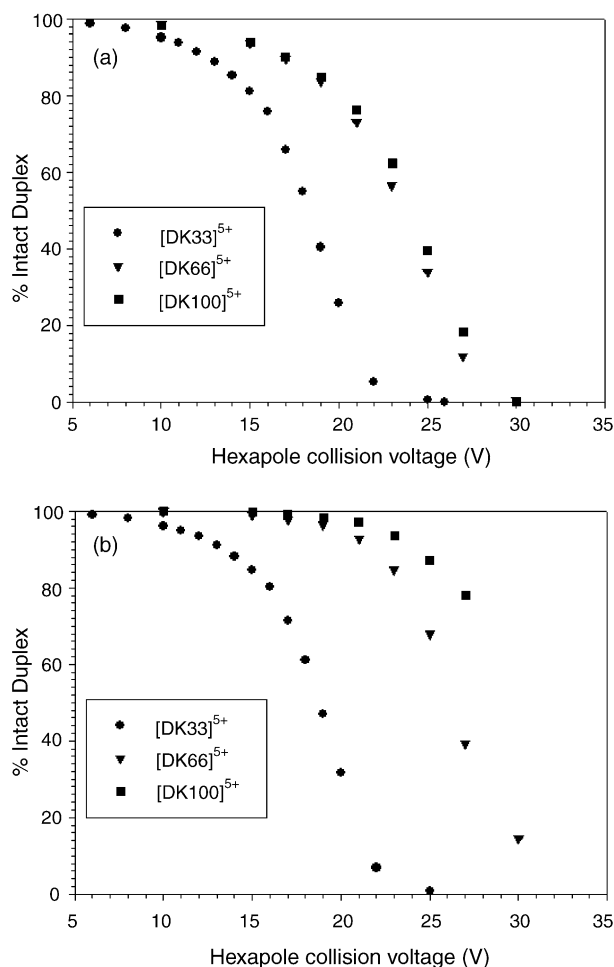


Fig. 7. Dissociation curves obtained on duplex $[\text{Dk33}]^{5+}$ (circles), duplex $[\text{Dk66}]^{5+}$ (triangles down) and $[\text{Dk100}]^{5+}$ (squares) in positive ion mode. (a) The percentage of intact duplex relative to the sum of all fragments was calculated using Eq. (5a). (b) The percentage of intact duplex relative to the fragmentation into single strands (path (i) in Eq. (4)) was calculated using Eq. (5b).

of the percentage of intact duplex.

$$\% \text{ Intact duplex} = \frac{I(\text{duplex}^{5+}) \times 100\%}{I(\text{duplex}^{5+}) + (I(\text{ss}^{3+}) + I(\text{ss}^{2+}))/2} \quad (5b)$$

The results, presented in Fig. 7(b), suggest that the Watson–Crick hydrogen bonds are conserved in the protonated duplexes [28,29]. It must be noted that the curve shape and order does not depend on the fact that we divide the contribution of the fragments by two when one parent ion results in two charged fragments.

The next question is whether the stacking interactions are conserved or not in the double-stranded DNA detected in the positive ion mode. As we did previously in the negative ion mode [29], we performed MS/MS experiments on 16-mer duplexes each containing eight GC and eight AT base pairs, but with various sequences. In the negative ion mode, the collision voltage needed to provoke 50% of dissociation was correlated with the enthalpy of formation of the duplex in solution, calculated using a nearest-neighbor model. Table 3 summarizes the base sequences of the [duplex + 7H]⁷⁺ (strands A and B have different masses), the enthalpy of formation in solution calculated using a nearest-neighbor model [36], and the collision voltage at which 50% of dissociation is observed. The percentage of intact duplex is calculated using Eq. (6).

%Duplex

$$= \frac{I(\text{AB}^{7+}) \times 100\%}{I(\text{AB}^{7+}) + ((I(\text{A}^{3+}) + I(\text{B}^{4+}) + I(\text{A}^{4+}) + I(\text{B}^{3+}))/2)} \quad (6)$$

In the negative ion mode, the gas-phase kinetic stability of duplexes **1**, **2** and **3** follows the nearest-neighbor predictions. Only duplex **4** is less stable than predicted, but it is well known that A-tract sequences destabilize duplexes by bending [37,38], as discussed previously [29]. Positive ion mode results on [duplex + 7H]⁷⁺ (this work, Table 3) agree less well with this picture: duplex **3** is now as stable as duplex **1**, and the A-tract duplex **4** is not as destabilized as in the negative ion mode and as in solution.

Overall, the MS/MS results on duplex DNA in positive mode suggest that hydrogen bonding is conserved, but that the confor-

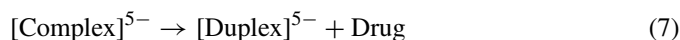
mation of the duplexes (responsible for base stacking, or A-tract destabilization interactions) is not conserved in the protonated duplexes. This recalls the behavior of the duplex–drug complexes in positive ion mode. The purely intercalating complexes, stabilized by stacking interactions only, are not observable in positive ion mode, indicating that stacking interactions are not conserved in the positively charged DNA complexes. However, complexes with ligands possessing hydrogen bonds with the DNA bases are still observed in positive ion mode, indicating that hydrogen bonding interactions are preserved in positive ion mode.

3.3. MS/MS on DNA–drug complexes in the negative ion mode

In MS/MS, the amount of intact complex at a given hexapole collision voltage depends on the fragmentation kinetics, i.e., on the activation enthalpy and on the activation entropy. If we want to correlate the breakdown curves with the activation enthalpy, which itself correlates with the interaction energy between the fragmenting partners, we need to compare channels of similar activation entropy. Therefore, we first classify the drugs in three groups, according to the preferred dissociation pathway of their complexes. The whole discussion below holds for the dissociation of the 1:1 complex [duplex + ligand]⁵⁻ with the duplexes Dk33, Dk66, and Dk100.

3.3.1. Group 1: loss of neutral drug

The first group includes the ligands for which the complex dissociates mainly via the loss of neutral drug. The dissociation pathway is:



Daunomycin, doxorubicin, *m*-Amsacrine, ellipticine, proflavine, mitoxantrone, cryptolepine and neocryptolepine belong to this group. All of them are intercalators. The case of daunomycin and doxorubicin will be described in more detail. Fig. 8 shows the MS/MS spectra of the [complex]⁵⁻ formed between the duplex d(CGCGAATTCGCG)₂ (Dk66) and (a) daunomycin, or (b) doxorubicin. At hexapole collision voltage of 24 V, the complex with daunomycin is more dissociated than with doxoru-

Table 3

Test for the conservation of stacking interactions in the gas phase: collision-induced dissociation of 16-mer duplexes containing eight AT and eight GC base pairs

	Sequence	ΔH_{n-n} [36] (kcal/mol)	CE (50%) [duplex] ⁷⁺ (eV)	CE (50%) [29] [duplex] ⁷⁻ (eV)	CE (50%) [29] [duplex] ⁶⁻ (eV)
1	5'-AAATCGCGGCGCTAAA-3' 3'-TTTAGCGCCGCGATT-5'	-136.8	20.4	13.6	24.5
2	5'-GGGCTATAATATCGGG-3' 3'-CCCGATATTATAGCCC-5'	-125.3	19.0	13.1	21.1
3	5'-AGACTGTGAGTCAGTG-3' 3'-TCTGACACTCAGTCAC-5'	-122.6	20.3	12.3	20.1
4	5'-GGGCTTTTAAACGGG-3' 3'-CCCGAAAATTTGCC-5'	-135.9 ^a	19.8	13.0	20.1

^a This value does not reflect solution-phase stability because of particular structures adopted by A-tract DNAs [37,38].

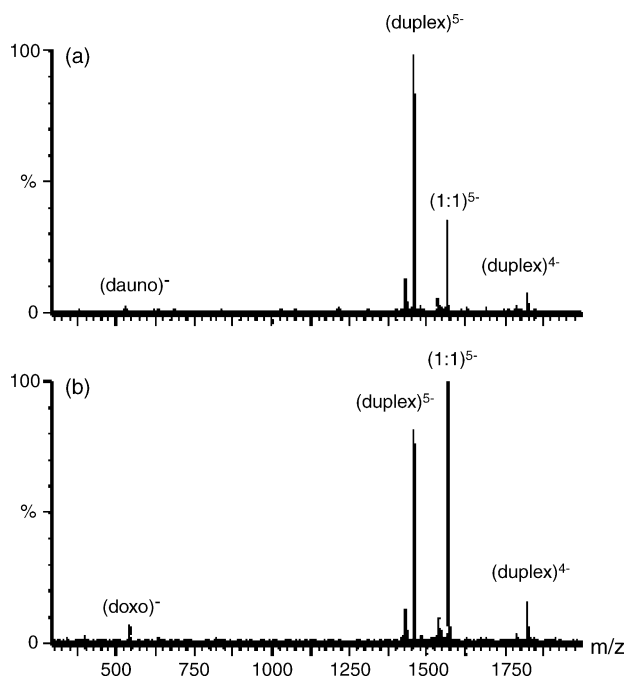


Fig. 8. Negative ion mode MS/MS spectra of (a) the daunomycin-Dk66 (1:1)⁵⁻ complex ($m/z = 1564.9$) and (b) the doxorubicin-Dk66 (1:1)⁵⁻ complex ($m/z = 1568.1$) at 24 V hexapole collision voltage. The most abundant resulting fragment is the (duplex)⁵⁻ ($m/z = 1459.4$). The minor fragments are (duplex)⁴⁻ and the deprotonated drug.

bicin. The resulting fragment is the [duplex]⁵⁻. Small amounts of [duplex]⁴⁻ and [drug]⁻ are also observed. These fragments are minor, but are taken into account in the calculation of the percentage of intact complex by using Eq. (8).

$$\% (\text{Intact complex}) = \frac{I(\text{complex}^{5-}) \times 100\%}{\{I(\text{complex}^{5-}) + I(\text{duplex}^{5-}) + I(\text{duplex}^{4-}) + I(\text{drug}^{-})\}/2} \quad (8)$$

When comparing complexes fragmenting via the same pathway, the collision voltage required for fragmentation is directly linked to the activation energy. We can use comparisons between drugs

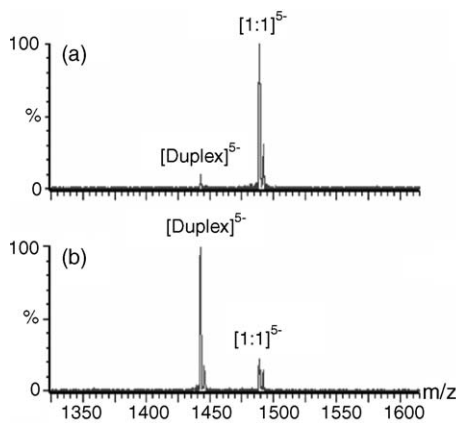
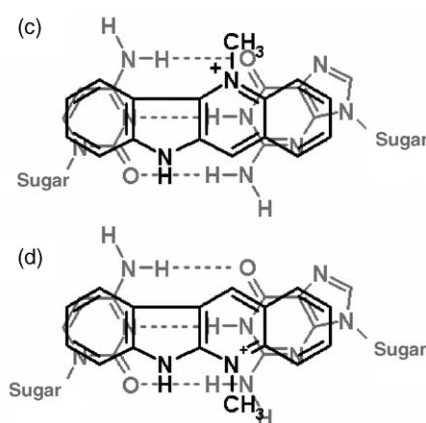


Fig. 9. Negative ion mode MS/MS spectra of the complex [1:1]⁵⁻ of duplex Dk66 with (a) cryptolepine and (b) neocryptolepine at the same hexapole collision voltage (10 V); the resulting fragment is the [duplex]⁵⁻. Superimposition of the chemical structures of a CG base pair (grey) and of (c) cryptolepine or (d) neocryptolepine (drug) in black). Structure (d) shows unavoidable steric clash between the methyl group of neocryptolepine and a NH₂ group of the base pair.

for a given duplex to assess the drug interaction energy with the duplex. In Fig. 8 we see that at a given hexapole collision voltage the complex with doxorubicin is more kinetically stable than the complex with daunomycin, and one can conclude that the activation enthalpy for dissociation is higher for the complex with doxorubicin. The difference in activation enthalpy is consistent with the extra hydrogen bond present in the doxorubicin complex due to the extra OH group [7,32]. This example illustrates a case where ESI-MS allows probing subtle differences in the drug–DNA intermolecular interactions. Another successful case is that of cryptolepine and neocryptolepine. These positional isomers have different binding affinities in solution, with cryptolepine having higher binding constants than neocryptolepine [39,40]. MS/MS was performed for both complexes with Dk66. Fig. 9(a and b) shows the MS/MS spectra obtained at collision voltage of 10 V for both complexes. Clearly the complex with neocryptolepine dissociates faster than the complex with cryptolepine, thereby reflecting the solution-phase binding affinity. It can therefore be concluded that the difference in binding affinity in solution is due to specific intermolecular interactions. The crystallographic structure of cryptolepine intercalated between GC base pairs has been published [41]. The schematic superimposition of the chemical structures of a GC base pair and of cryptolepine and neocryptolepine is shown in Fig. 9(c) and (d), respectively. In the case of cryptolepine (Fig. 9(c)), the NH group and the N–CH₃ group are on opposite sides of the molecule, and each one can therefore interact with a C=O group of the base pair. In the case of neocryptolepine (Fig. 9(d)), one of these interactions is lost, but in addition a steric hindrance occurs between the N–CH₃ group of neocryptolepine and one of the NH₂ groups of the base pairs.

Other useful information comes from the comparison between the breakdown curves obtained for a given drug and different duplexes, provided that the duplexes have the same size [42]. This is shown in Fig. 10(a) for doxorubicin and Fig. 10(b) for *m*-Amsacrine. Here the percentage of GC base pairs is changed, and all duplexes are 12-mers. In the case of doxorubicin, the complex with the duplex Dk33 dissociates via the separation of the single strands, so the breakdown curve can



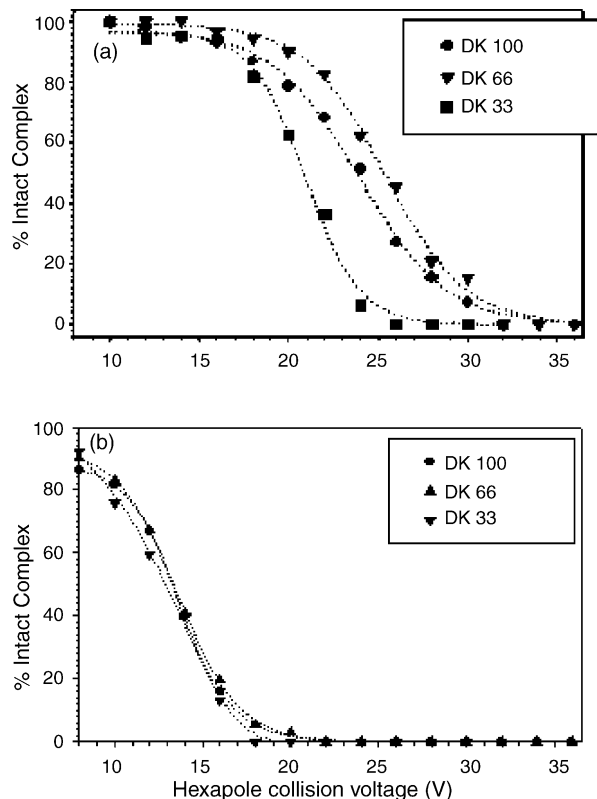


Fig. 10. Negative ion mode dissociation curves obtained on the $[1:1]^{5-}$ complexes between duplex Dk33 (circles), duplex Dk66 (triangles down) and Dk100 (squares) and (a) the drug doxorubicin or (b) the drug *m*-Amsacrine. The % of intact complex is calculated using Eq. (8).

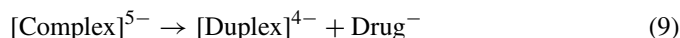
actually not be compared with those of Dk66 and Dk100, where the complex fragments via the loss of neutral drug. The data in Fig. 10(a) indicate that the complex formed with Dk66 is more stable in the gas phase than the complex with Dk100. This suggests that doxorubicin interacts more strongly in the gas phase with the duplex when some AT base pairs are present. This is consistent with the sequence preference found in solution phase [43–45], and suggests that the MS/MS approach is in the present case valid for probing subtle changes in interaction strength.

A contrasting example is given by the drug *m*-Amsacrine (Fig. 10(b)). Here the complexes dissociates via the loss of neutral drug for all three duplexes, so the three curves can be compared directly. Their superimposition suggests that, although the base sequence (and GC content) differs, the interaction energy is the same for all three duplexes. Either the binding site is the same (*m*-Amsacrine could intercalate between the last GC base pairs of the duplex), or the interaction energy between the three duplexes and the drug is very similar whatever the binding site on the duplex. *m*-Amsacrine is an intercalator [46,47] with a preference for GC base pairs. In full scan ESI-MS, the relative amount of complex depends directly on the GC base pair content. Taken together, the ESI-MS and MS/MS results suggest that *m*-Amsacrine interacts with GC sites only.

3.3.2. Group 2: loss of deprotonated drug

The second group includes drugs for which the complex dissociates via the loss of a negatively charged drug (Eq. (9)).

Actinomycin D is here the only representative of this group.



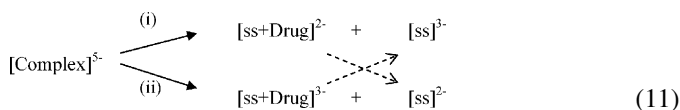
The percentage of intact complex is therefore calculated using Eq. (10).

$$\begin{aligned} \% (\text{Intact complex}) &= \frac{I(\text{complex}^{5-}) \times 100\%}{I(\text{complex}^{5-}) + (I(\text{duplex}^{4-}) + I(\text{drug}^-))/2} \quad (10) \end{aligned}$$

Fig. 11(a) shows an MS/MS spectrum obtained with a hexapole collision voltage of 28 V for the duplex d(CGCGAATTCGCG)₂ and actinomycin D. Losses of base G are also observed, but to a much lesser extent than in ion trap MS/MS [24,28]. Again, the comparison between the breakdown curves (Fig. 11(b)) obtained with the Dk66 and Dk100 duplex suggests that the complex is more stabilized with the duplex containing some AT base pairs (Dk66), which would be consistent with the interaction between the bulky peptidic group of actinomycin lying in the minor groove and making better contacts with AT than with GC base pairs [9,48]. However, as the drug gives a proton to the duplex, one cannot exclude that the difference in breakdown curves is due to a different proton affinity between $[\text{Dk66}]^{4-}$ and $[\text{Dk100}]^{4-}$ (see also discussion below for positive ion mode).

3.3.3. Group 3: drug remaining attached to the single strands

The third group includes drugs for which the complex dissociates via the separation into the single strands (noted ss) which share the available charges, and some drug molecule can stick on both strands (Eq. (11)). The positively charged intercalator ethidium (Fig. 1), and all minor groove binders (Fig. 2) belong to this group. This dissociation channel is the same as for the duplex alone (separation into single strands). Usually reaction path (i) is more favored than path (ii). In the case of Hoechst 33258 and 33342, loss of neutral drug from the single strands is also possible, as the intensity of the single strands without drug is somewhat larger than the intensity of single strands with drugs. Eq. (12) is used to calculate the breakdown curves.



$$\begin{aligned} \% (\text{Intact complex}) &= \frac{I(\text{complex}^{5-}) \times 100\%}{\{I(\text{complex}^{5-}) + (I(\text{ss}^{3-}) + I(\text{ss}^{2-}) \\ &\quad + I([\text{ss} + \text{drug}]^{3-}) + I([\text{ss} + \text{drug}]^{2-}))/2\}} \quad (12) \end{aligned}$$

In the case of minor groove binders, the magnitude of the hexapole collision voltage needed to fragment the complex reveals that the complex is more stable than the duplex alone (Fig. 12). The results obtained with a non-self complementary duplex and Hoechst 33258 and netropsin have been previously

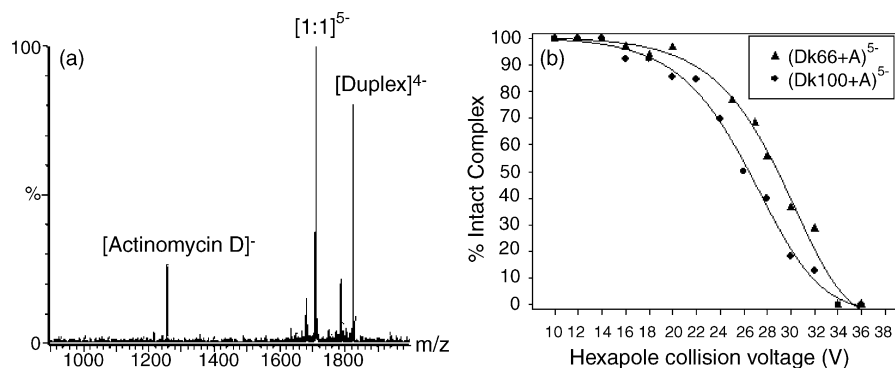


Fig. 11. (a) Negative ion mode MS/MS spectrum of the $[1:1]^{5-}$ complex between duplex Dk66 and actinomycin D ($m/z = 1709.6$) at hexapole collision voltage of 28 V. The fragments are the $[\text{duplex}]^{4-}$ ($m/z = 1823.3$) and $(\text{actinomycin D})^{-}$ ($m/z = 1255.7$). (b) Negative ion mode MS/MS dissociation curves of actinomycin D with the $d(\text{CGCGAATTCGCG})_2$ (Dk66) duplex (triangles up) and the duplex $d(\text{CGCG}_3\text{C}_3\text{GC})_2$ (Dk100) (circles). The % of intact complex is calculated using Eq. (10).

described [22]. We have shown that the dissociation channel observed could reflect some structural features of these two drugs. The complex with netropsin is kinetically more stable than the complex with Hoechst 33258 because it forms more hydrogen bonds with the duplex. Fig. 12 shows the results obtained with the self-complementary duplexes Dk66 and Dk33. Again, the complex with netropsin dissociates at higher collision voltage than that with Hoechst 33258. The complex with Hoechst 33342 is slightly less stable than the complex with Hoechst 33258. The interaction with the binding site is probably less favorable due to the substitution of the hydroxyl group by a methoxy for Hoechst 33342.

The number of hydrogen bonds formed between the duplex and the drugs is not the only reason of the stabilization of the duplex observed. The number of positive charges carried by the drugs influences the stability of the complex due to electrostatic interactions. Netropsin and DAPI have two positive charges compared to one for Hoechst 33258 and 33342. The duplex will be more stabilized with DAPI than with the Hoechst drugs even if less hydrogen bonds between the duplex and the drug are present.

To summarize the MS/MS results in the negative ion mode, the charge of the drug is the major factor influencing the fragmentation pathway, even more than the binding mode (intercalation or minor groove binding). The information that can be extracted from the MS/MS experiments depends on the fragmen-

tation pathway. When the neutral drug is lost upon fragmentation of the complex, it may be possible to correlate the collision voltage required for dissociation to the intermolecular binding energy (drug–duplex interactions). However, for positively charged drugs like those in Group 3, it is impossible to probe the strength of drug–duplex interactions directly. Only the reinforcement of the interactions between the two single strands can be probed. The fragmentation pathways are more simple in a Q-TOF than in a quadrupole ion trap mass spectrometer. In quadrupole ion trap, due to the lower excitation energies and longer activation times, neutral base loss occurs at lower apparent collision energies compared to the other channels. As a result, only the very loosely bound drugs which get off as neutrals, or complexes with fragile duplexes like Dk33, give the same fragmentation pattern as on the Q-TOF. The other complexes show primarily base loss.

3.4. MS/MS on DNA-drug complexes in the positive ion mode

We also explored the possibilities of MS/MS experiment on complexes produced in the positive ion mode, for the ligands that showed a complex. The goal was two-fold. First, we wanted to address the problem of the maintenance of specific interactions like hydrogen bonds in the positively charged complexes, in order to complement our observations in full scan ESI-MS. The

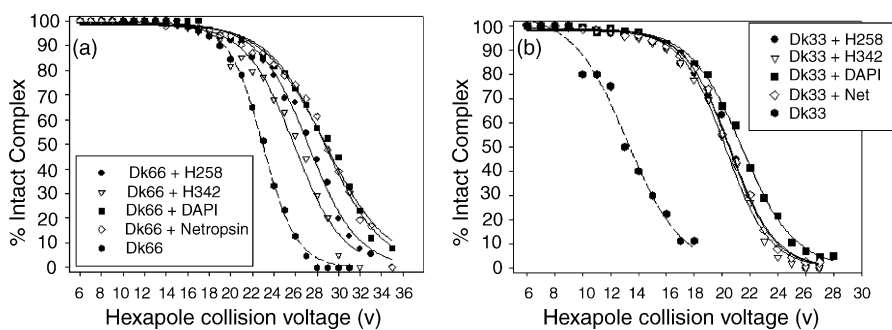


Fig. 12. Negative ion mode MS/MS dissociation curves of the duplexes (a) Dk66 and (b) Dk33 and their complexes with minor groove binders. The % of intact complex is calculated using Eq. (12). Symbol key: black hexagons = $[\text{duplex}]^{3-}$; white diamonds = $[1:1]^{5-}$ complex with netropsin; black squares = $[1:1]^{3-}$ complex with DAPI; white triangles down = $[1:1]^{5-}$ complex with Hoechst 33342; black circles = $[1:1]^{3-}$ complex with Hoechst 33258.

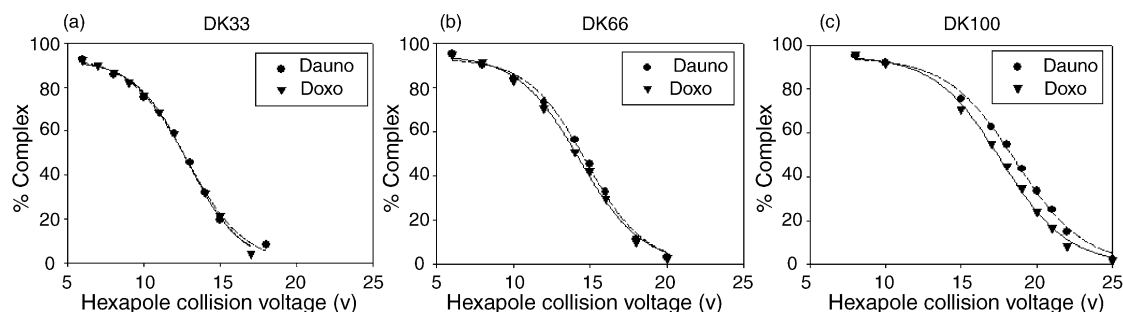


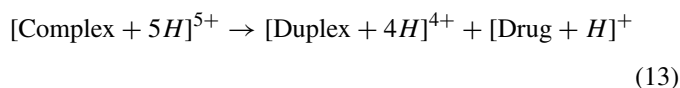
Fig. 13. Positive ion mode MS/MS dissociation curve of the $[1:1]^{5+}$ complexes between duplexes (a) Dk33; (b) Dk66; and (c) Dk100 with the drugs daunomycin (circles) and doxorubicin (triangles down). The % of intact complex is calculated using Eq. (14).

two intercalators daunomycin and doxorubicin, which differ by a single hydrogen bond, are adequate test molecules. Second, we wanted to test whether positive ion mode MS/MS would allow to get complementary information on the drug–duplex interactions in the case of positively charged drugs, which remain attached on the single strands in negative ion mode MS/MS.

3.4.1. Daunomycin and doxorubicin

We have seen that, in the negative ion mode, the higher stability of the complex with doxorubicin strongly suggested that the extra hydrogen bond was conserved in the gas-phase complex. We also showed in full scan ESI-MS that these two intercalators are some of the few for which a complex can be observed in positive ion mode. Therefore, it is an interesting study case to test whether the desolvated complexes in the positive ion mode have conserved or not the doxorubicin extra hydrogen bond present in solution.

For daunomycin and doxorubicin, the complex dissociates in the positive ion mode primarily via the loss of singly protonated drug.



The drug can also further fragment via the loss of the daunosamine sugar. In the case of the duplex Dk33, some dissociation of the duplex into single strands can be observed at high collision voltage. Fig. 13 shows the dissociation curves obtained for the intercalators daunomycin and doxorubicin. The percentage of intact complex is calculated using Eq. (14), where $I(\text{drug}^+)$ stands for the intensities of the peak of the drug (plus the intensity of the peak of the fragment of the drug in the case of daunomycin and doxorubicin).

$$\begin{aligned} \% (\text{Intact complex}) \\ = \frac{I(\text{complex}^{5+}) \times 100\%}{I(\text{complex}^{5+}) + (I(\text{duplex}^{4+}) + I(\text{drug}^+))/2} \quad (14) \end{aligned}$$

The dissociation curves obtained with the duplex Dk33 are superimposed for the two drugs. For the duplexes Dk66 and Dk100, the stability of the complex with daunomycin is slightly higher than with doxorubicin. This behavior contrasts with that observed in the negative ion mode (Fig. 8), where the desolvated complex with doxorubicin was more stable, and also disagrees

with the solution-phase data [7] where the doxorubicin complex is stabilized by one more hydrogen bond than the complex with daunomycin.

Two hypotheses can be raised: either the geometry of the intercalation complex is modified during the electrospray process in the positive ion mode, so that the extra hydrogen bond of doxorubicin is no longer present, or there is another factor that lowers the activation enthalpy of dissociation of the complex with doxorubicin. In positive ion mode, the fragmentation proceeds via the loss of a protonated drug. Therefore, one should consider the $[\text{DNA} + \text{drug} + nH]^{n+}$ complex as proton-bound complex, and one factor that will influence the stability of the dissociation products when comparing two drugs is the proton affinity of the drug. The higher the proton affinity, the easier it is for the drug to leave as $[\text{drug} + H]^+$.

The proton affinity of the drug is defined as $-\Delta H^\circ$ for the reaction: $\text{Drug} + H^+ \rightarrow \text{DrugH}^+$. The drug proton affinities at all possible sites of protonation (see the numbering of the sites in Fig. 3) were calculated at the semi-empirical AM1 level of theory [49], and the results are shown in Table 4. The site of highest proton affinity, i.e., the most favored protonation site is the NH_2 group on the sugar. The calculations give a higher proton affinity for doxorubicin than for daunomycin. So, the fact that doxorubicin complex is less stable in the positive mode does not necessarily indicate that the extra hydrogen bond is absent in the positively charged complex, because it could as well be a

Table 4
Proton affinities of doxorubicin and daunomycin calculated at the AM1 semi-empirical level of theory

Doxorubicin	PA (kcal/mol)	Daunomycin	PA (kcal/mol)
Site 1 (N)	231.9	Site 1 (N)	229.5
Site 2 (OH)	192.7	Site 2 (OH)	190.8
Site 3 (O)	204.8	Site 3 (O)	202.8
Site 4 (O)	207.6	Site 4 (O)	208.5
Site 5 (OH)	194.1	Site 5 (OH)	200.0
Site 6 (OH)	188.3	–	–
Site 7 (CO)	187.3	Site 7 (CO)	192.7
Site 8 (OH)	178.2	Site 8 (OH)	179.9
Site 9 (CO)	197.2	Site 9 (CO)	198.6
Site 10 (O)	184.7	Site 10 (O)	186.0
Site 11 (O)	214.2	Site 11 (O)	215.7
Site 12 (OH)	188.7	Site 12 (OH)	192.4

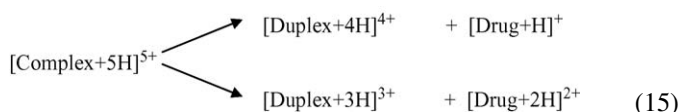
Protonation sites are defined in Fig. 3.

PA effect. We can therefore not conclude on the persistence of the conformation of the intercalation site.

There is another striking difference between positive and negative ion mode in the comparison of the three duplexes. In negative ion mode the relative stability of the complex ranks Dk66 > Dk100 > Dk33. In positive ion mode however it ranks Dk100 > Dk66 > Dk33. Again, this could reflect the different proton affinities of the duplexes rather than preferential binding of the drug for GC base pairs. PA's of nucleoside monophosphates have been reported [35]. Purines (G and A) have a higher PA than pyrimidines (C and T), and guanine has slightly higher PA's than adenine. This is consistent with higher activation energy with Dk100 (12 guanines), because it requires more energy to transfer a proton from the duplex to the drug.

3.4.2. Complexes with minor groove binders

In the positive ion mode, the complexes with minor groove binders dissociate primarily via the loss of singly or doubly protonated drug:



The relative intensities of the different species observed in the mass spectra are calculated using the following equations:

$$\begin{aligned} \% (\text{Intact complex}) &= \frac{I(\text{parent}^{5+}) \times 100\%}{\{I(\text{parent}^{5+}) + (I(\text{duplex}^{4+}) + I(\text{drug}^+) + I(\text{duplex}^{3+}) + I(\text{drug}^{2+}))/2\}} \quad (16) \end{aligned}$$

$$\% \text{Drug}^+ = \frac{(I(\text{duplex}^{4+}) + I(\text{drug}^+))/2 \times 100\%}{\{I(\text{parent}^{5+}) + (I(\text{duplex}^{4+}) + I(\text{drug}^+) + I(\text{duplex}^{3+}) + I(\text{drug}^{2+}))/2\}} \quad (17)$$

$$\% \text{Drug}^{2+} = \frac{(I(\text{duplex}^{3+}) + I(\text{drug}^{2+}))/2 \times 100\%}{\{I(\text{parent}^{5+}) + (I(\text{duplex}^{4+}) + I(\text{drug}^+) + I(\text{duplex}^{3+}) + I(\text{drug}^{2+}))/2\}} \quad (18)$$

Fig. 14 shows the evolution of the relative intensities of the different species observed in positive ion mode MS/MS spectra. The left column shows the results obtained for the Dk33 d(CGTA₃T₃ACG)₂ duplex and the right column shows the results with the Dk66 d(CGCGAATTCGCG)₂ duplex complexed with the minor groove binders.

Netropsin leaves the duplex exclusively with two positive charges. For the other ligands, the tendency to leave as doubly charged ranks as follows: Hoechst 33342 ≥ Hoechst 33258 > DAPI. This behavior can again be explained with the proton affinities of the drugs. In the literature, Hoechst 33258 and 33342 are usually represented with one positive charge; while DAPI and Netropsin are usually represented with two positive charges, and this corresponds to the preferred form in solution at pH 7 [50]. In Fig. 1 we gave the structure of the corresponding neutrals species for clarity. We then have calculated

the proton affinities of the neutral drugs for all possible protonation sites, and then the proton affinities of the singly protonated drugs, to deduce which one has the greatest tendency to take two protons. The results are shown in Table 5.

Despite the modest level of theory used for the calculations of the PA's, the results agree quite well with the observations. Singly protonated netropsin has indeed the highest proton affinity, i.e., the highest tendency to take a second proton. Protonated DAPI has the lowest proton affinity, consistent with its very low tendency to take away a second proton from the complex upon fragmentation. Hoechst 33258 and 33342 have similar proton affinities, between the netropsin and DAPI. Looking at Eq. (15), we can see the two reaction channels as a competition between [duplex + 3H]³⁺ and [drug + H]⁺ for taking the fifth proton. This description is based on the same principles as the Cooks' kinetic method [51,52]. From the dissociation curves in Fig. 14, we can therefore deduce that the proton affinity of [duplex + 3H]³⁺ must lie between that of [DAPI + H]⁺ and that of [netropsin + H]⁺. Similarly, when comparing duplexes Dk33 and Dk66, one can see that the tendency for the drug to leave as a doubly charged species is slightly higher for Dk33, consistent with a higher proton affinity for [Dk66 + 3H]³⁺.

Fig. 15 shows the dissociation curves obtained for each minor groove binder and the duplex Dk66. The percentage of intact complex is calculated using the Eq. (16). The activation energies for dissociation of the different complexes are in the order: H258 > H342 > DAPI > netropsin. However, the interpretation of this ranking is now very difficult because the activation enthalpy depends on at least three parameters: (1) the strength of the noncovalent interactions between the drug and the duplex, which we would like to probe, but also (2) the effect of the drug proton affinity and (3) the fact that the dissociation channel giving duplex³⁺ + drug²⁺ is characterized by a higher coulombic repulsion between the fragments. This latter factor explains at least why the complex with netropsin (fragmenting exclusively by loss of drug²⁺) has the lowest activation energy.

Table 5
Proton affinities of the minor groove binders calculated at the AM1 semi-empirical level of theory

	PA _{neutral} (kcal/mol)	PA _{charged} (kcal/mol) ^a
Hoechst 33342	Site 1: 218.9	Site 2: 191.4 Site 3: 203.6 Site 4: 161.4 Site 5: 174.6 Site 6: 160.8
Hoechst 33258	Site 1: 215.4	Site 2: 193.8 Site 3: 204.6 Site 4: 152.4 Site 5: 176.1 Site 6: 163.2
DAPI	Site 1: 241.6 Site 2: 237.2	Site 2: 199.9
Netropsin	Site 1: 243.1 Site 2: 236.7	Site 2: 213.4

The sites of protonation on the molecule are numbered in as in Fig. 1.

^a PA of the ligand already protonated on site 1.

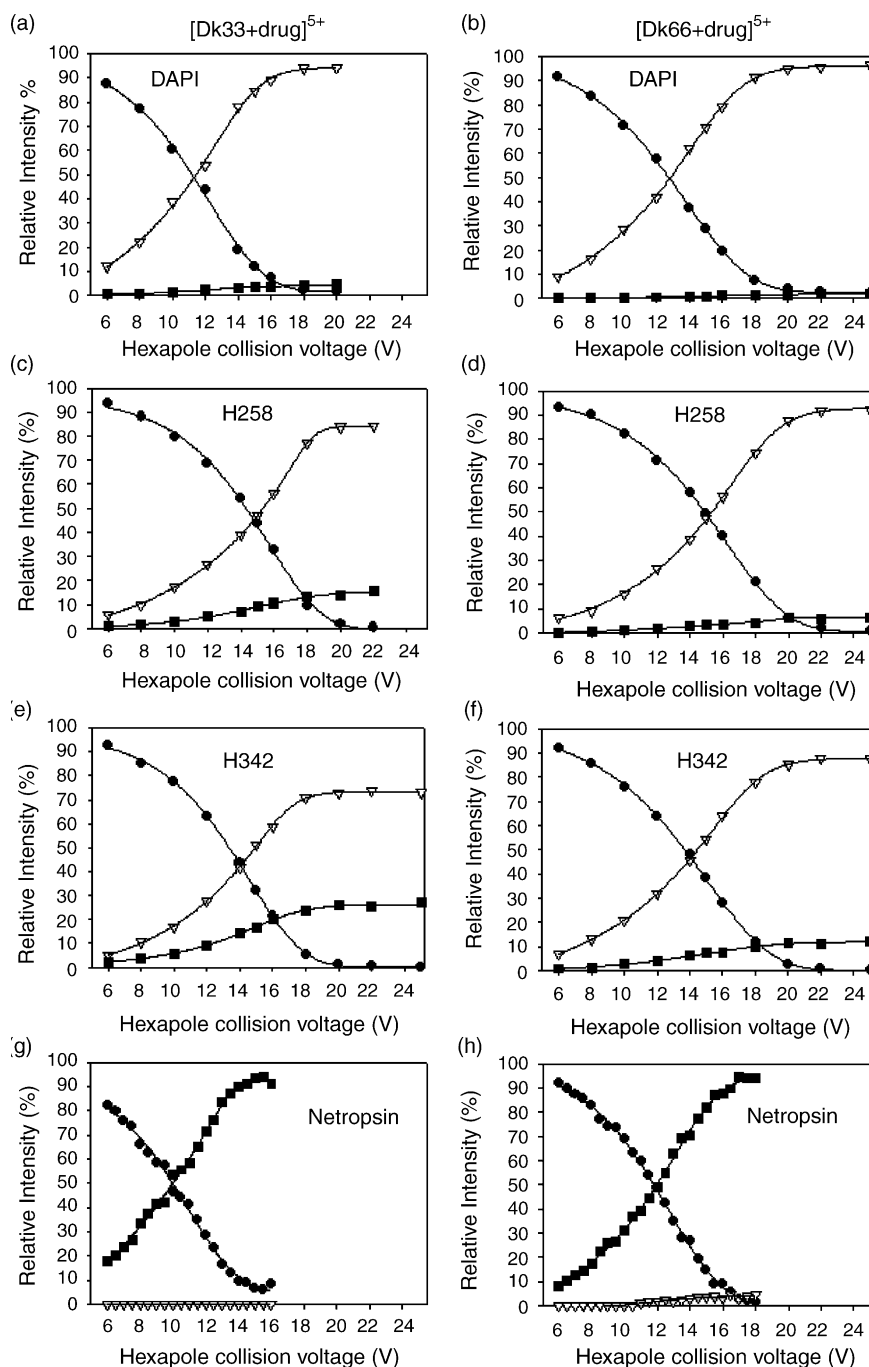


Fig. 14. Positive ion mode MS/MS on the [1:1]⁵⁺ complexes with minor groove binders; (a) [Dk33 + DAPI]⁵⁺; (b) [Dk66 + DAPI]⁵⁺; (c) [Dk33 + Hoechst 33258]⁵⁺; (d) [Dk66 + Hoechst 33258]⁵⁺; (e) [Dk33 + Hoechst 33342]⁵⁺; (f) [Dk66 + Hoechst 33342]⁵⁺; (g) [Dk33 + netropsin]⁵⁺; (h) [Dk66 + netropsin]⁵⁺. Symbol key: black circles = % of [1:1]⁵⁺ (calculated using Eq. (16)); open triangles down = % of drug⁺ (calculated using Eq. (17)); black squares = % of drug²⁺ (calculated using Eq. (18)).

This illustrates the difficulties of getting information on the noncovalent interactions by MS/MS in the positive ion mode.

4. General discussion and conclusions

4.1. On the use of positive ion mode ESI-MS

Our systematic comparison of positive and negative ion mode, with a wide panel of well-known duplex DNA lig-

ands, leads to the conclusion that the first choice in studying drug–DNA interactions should always be negative ion mode. All results presented here demonstrate that there are neither false positives, nor false negatives in the complexes observed in negative ion mode ESI-MS. In positive ion mode, there may be some false negatives, as has been shown by Sheil and co-workers [20,21] and in the present work for the intercalators that bind to duplex DNA exclusively by stacking interactions. At the most, positive ion mode could be used, when a complex

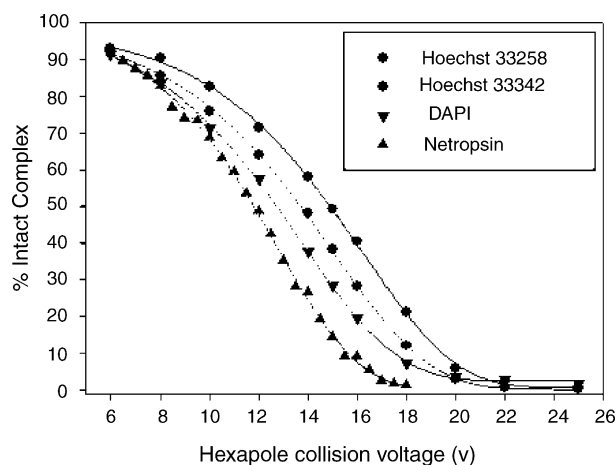


Fig. 15. Positive ion mode MS/MS dissociation curves obtained for the duplex $d(CGCGAATTCGCG)_2$ (Dk66) complexed with minor groove binders. The charge state selected was 5+. The percentage of intact complex was calculated using Eq. (16).

is detected in negative ion mode, to test whether the complex involved purely stacking interactions or whether there are other hydrogen bonding interactions remaining.

4.2. On the interpretation of MS/MS data

MS/MS data contain basically two kinds of information: the fragmentation channel (the nature of the fragments observed) and the collision voltage at which fragmentation occurs. The mass spectrometrists' hope is generally that MS/MS will give some insight into the ligand binding mode, and binding energy.

4.2.1. Information on ligand binding mode

In the literature we very often encounter the concept that the ligand binding mode can be deduced from the fragmentation channel in MS/MS [24,53]. For example, Wan et al. [24] observed on a quadrupole ion trap that complexes with minor groove binders dissociate via neutral base loss and covalent breaking of the oligonucleotide, while complexes with intercalators dissociate via noncovalent bond breaking giving the duplex and/or the single strands. The concept is sensible, but it must be kept in mind that several other factors than the binding mode can influence the fragmentation channel(s) observed in MS/MS:

- (1) The choice of the instrument. We have shown before [28] that neutral base loss was favored at low collision energies (long dissociation times) such as encountered in a quadrupole ion trap, and that noncovalent bond cleavage was favored at higher collision energies (short dissociation time) such as in a Q-TOF. Drawing conclusions based on the presence or absence of base loss is therefore hasty.
- (2) The charge state of the selected ion. A high charge state involves a higher coulombic repulsion, and the dissociation channels provoking the fragmentation in charged species will be favored [26,29]. Lower charge states will be more prone to neutral base loss.

- (3) The proton affinity of the drug. We have demonstrated here that the distinction between intercalation and minor groove binding is not reliable if based only on the dissociation channel, as the intercalator ethidium behaves like the minor groove binders in negative ion mode MS/MS. The same was observed in an LCQ quadrupole ion trap mass spectrometer (data not shown). If we classify the drugs according to the fragmentation channel observed in negative mode, the three groups correlate more with the drug proton affinity than with the binding mode. The fact that most minor groove binders are positively charged in solution and that most intercalators are neutral in solution may have led to the erroneous impression that dissociation channel could be indicative of the ligand binding mode.

4.2.2. Information on ligand binding energy

Until now, the only cases where we unambiguously have a correlation between the intermolecular interactions and the gas-phase dissociation kinetics involve dissociation via neutral drug loss. In the case of daunomycin and doxorubicin in the negative mode, our results agree very well with the $\Delta G^\circ_{\text{mol}}$ determined by Chaires et al. [7], illustrating the power of MS/MS to probe $\Delta G^\circ_{\text{mol}}$ experimentally. Neutral drug loss is observed only with some intercalators in the negative ion mode. Also, it must be noted that this channel can only be observed for weakly binding intercalators and stable duplexes; else other fragmentation channels occur, such as the dissociation of the duplex itself. In the cases where fragmentation implies a gas-phase proton transfer between the duplex and the drug, it is very likely that the kinetic stability in MS/MS will rather reflect the relative gas-phase proton affinities (positive ion mode) or gas-phase basicities (negative ion mode) of the duplex and the drug. Another point to consider for the comparison between ligands is the reaction mechanism. Even if the nature of the fragments is similar, different reaction mechanisms (i.e., rearrangements) could be at stake in the dissociation. Rearrangements are very likely when the site or degree of protonation is not the same in the gas phase as in the solution from which the complex was extracted. In the future, a joint use of ESI-MS/MS experiments and theoretical calculations could help getting insight into the complex geometry, but this area needs further development, both on the experimental and on the theoretical point of view. As MS/MS is sensitive to the dissociation kinetics, theory and experiments can only be linked if the dissociation mechanism and all rate limiting steps can be modeled. In the current state of the art, MS/MS should be trusted only in the case of neutral drug losses, and for security only for the comparison of structurally similar ligands.

Acknowledgements

This work has been supported by the FNRS (Postdoctoral research fellowship to V.G., and FRFC grant number 2.4623.05), by the CART (Centre d'Analyse des Résidus en Traces, financed by the Walloon Region and by the European Social Funds), by the Walloon Region project NOMADE, and by the University of Liège (Action de Recherche Concertée ARC n° 99/04–245). VG is now FNRS Research Associate.

References

- [1] B. Ganem, Y.-T. Li, J.D. Henion, *J. Am. Chem. Soc.* 113 (1991) 6294.
- [2] R.D. Smith, K.J. Light-Wahl, *Biol. Mass Spectrom.* 22 (1993) 493.
- [3] R.D. Smith, J.E. Bruce, Q. Wu, Q.P. Lei, *Chem. Soc. Rev.* 26 (1997) 191.
- [4] J.M. Daniel, S.D. Friess, S. Rajagopalan, S. Wendt, R. Zenobi, *Int. J. Mass Spectrom.* 216 (2002) 1.
- [5] E.N. Kitova, D.R. Bundle, J.S. Klassen, *Angew. Chem. Int. Ed.* 43 (2004) 4183.
- [6] J.B. Chaires, *Anticancer Drug Des.* 11 (1996) 569.
- [7] J.B. Chaires, S. Satyanarana, D. Suh, I. Fokt, T. Przewloka, W. Priebe, *Biochemistry* 35 (1996) 2047.
- [8] J.B. Chaires, *Biopolymers* 44 (1997) 201.
- [9] J. Gallego, A.R. Ortiz, B. de Pascual-Teresa, F. Gago, *J. Comput. Aided Mol. Des.* 11 (1997) 114.
- [10] J. Ren, T.C. Jenkins, J.B. Chaires, *Biochemistry* 39 (2000) 8439.
- [11] J. Pindur, G. Fischer, *Curr. Med. Chem.* 3 (1996) 379.
- [12] B.H. Geierstranger, D.E. Wemmer, *Annu. Rev. Biomol. Struct.* 24 (1995) 463.
- [13] M.J. Waring, C. Bailly, *J. Mol. Recognit.* 7 (1994) 109.
- [14] A.H.J. Wang, *Curr. Opin. Struct. Biol.* 2 (1992) 361.
- [15] K.X. Wan, T. Shibue, M.L. Gross, *J. Am. Chem. Soc.* 122 (2000) 300.
- [16] F. Rosu, V. Gabelica, C. Houssier, E. De Pauw, *Nucleic Acids Res.* 30 (2002) e82.
- [17] F. Rosu, E. De Pauw, L. Guittat, P. Alberti, L. Lacroix, P. Mailliet, J.-F. Riou, J.-L. Mergny, *Biochemistry* 42 (2003) 10361.
- [18] K.A. Sannes-Lowery, R.H. Griffey, S.A. Hofstadler, *Anal. Biochem.* 280 (2000) 264.
- [19] K.A. Sannes-Lowery, J.J. Drader, R.H. Griffey, S.A. Hofstadler, *Trends Anal. Chem.* 19 (2000) 481.
- [20] R. Gupta, A. Kapur, J.L. Beck, M.M. Sheil, *Rapid Commun. Mass Spectrom.* 15 (2001) 2472.
- [21] R. Gupta, J.L. Beck, S.F. Ralph, M.M. Sheil, J.R. Aldrich-Wright, *J. Am. Soc. Mass Spectrom.* 15 (2004) 1382.
- [22] V. Gabelica, E. De Pauw, F. Rosu, *J. Mass Spectrom.* 32 (1999) 1328.
- [23] V. Gabelica, F. Rosu, C. Houssier, E. De Pauw, *Rapid Commun. Mass Spectrom.* 14 (2000) 464.
- [24] K.X. Wan, T. Shibue, M.L. Gross, *J. Am. Soc. Mass Spectrom.* 11 (2000) 450.
- [25] M. Reyzer, J.S. Brodbelt, S.M. Kerwin, D. Kumar, *Nucleic Acids Res.* 29 (2001) e103.
- [26] K.M. Keller, J.M. Zhang, L. Oehlers, J.S. Brodbelt, *J. Mass Spectrom.* 40 (2005) 1362.
- [27] K. Cimanga, T. De Bruyne, L. Pieters, A.J. Vlietinck, C.A. Turger, *J. Nat. Prod.* 60 (1997) 688.
- [28] V. Gabelica, E. De Pauw, *J. Am. Soc. Mass Spectrom.* 13 (2002) 91.
- [29] V. Gabelica, E. De Pauw, *Int. J. Mass Spectrom.* 219 (2002) 151.
- [30] <http://webbook.nist.gov/chemistry/ion/#GB>; accessed on 1 May 2005.
- [31] X. Qu, J.B. Chaires, *J. Am. Chem. Soc.* 123 (2001) 1.
- [32] J.B. Chaires, *Biophys. Chem.* 35 (1990) 191.
- [33] N.B. Cech, C.G. Enke, *Mass Spectrom. Rev.* 20 (2001) 362.
- [34] N.B. Cech, C.G. Enke, *Anal. Chem.* 73 (2001) 4632.
- [35] K.B. Green-Church, P.A. Limbach, *J. Am. Soc. Mass Spectrom.* 11 (2000) 24.
- [36] S.-I. Nakano, M. Fujimoto, H. Hara, N. Sugimoto, *Nucleic Acids Res.* 27 (1999) 2957.
- [37] D. MacDonald, K. Herbert, X. Zhang, T. Polgruto, P. Lu, *J. Mol. Biol.* 306 (2001) 1081.
- [38] D. Strahs, T. Schlick, *J. Mol. Biol.* 301 (2000) 643.
- [39] C. Bailly, W. Laine, B. Baldeyrou, M.-C. De Pauw-Gillet, P. Colson, C. Houssier, K. Cimanga, S. Van Miert, A.J. Vlietinck, L. Pieters, *Anticancer Drug Des.* 15 (2000) 191.
- [40] L. Dassonneville, A. Lansiaux, A. Wattelet, N. Wattez, C. Mahieu, S. Van Miert, L. Pieters, C. Bailly, *Eur. J. Pharmacol.* 409 (2000) 9.
- [41] J.N. Lisgarten, M. Coll, J. Portugal, C.W. Wright, J. Aymami, *Nat. Struct. Biol.* 9 (2002) 57.
- [42] V. Gabelica, E. De Pauw, *J. Mass Spectrom.* 36 (2001) 397.
- [43] C.A. Frederick, L.D. Williams, G. Ughetto, G.A. Van der Marel, J.H. Van Boom, A. Rich, A.H. Wang, *Biochemistry* 29 (1990) 2538.
- [44] H. Trist, D.R. Phillips, *Nucleic Acids Res.* 17 (1989) 3673.
- [45] A. Skorobogaty, R.J. White, D.R. Phillips, J.A. Reiss, *FEBS Lett.* 227 (1988) 103.
- [46] P.A. Cassileth, R.P. Gale, *Leukemia Res.* 10 (1986) 1257.
- [47] G. Fischer, J. Pindur, *Pharmazie* 54 (1999) 83.
- [48] F.-M. Chen, C. Liu, *Biochemistry* 35 (1996) 7283.
- [49] M.J.S. Dewar, E.G. Zoebisch, E.F. Healy, J.J.P. Steward, *J. Am. Chem. Soc.* 107 (1985) 3902.
- [50] M. Ladinig, W. Leupin, M. Meuwly, M. Respondek, J. Wirz, V. Zoete, *Helv. Chim. Acta* 88 (2005) 53.
- [51] R.G. Cooks, P. Wong, *Acc. Chem. Res.* 31 (1998) 379.
- [52] R.G. Cooks, J.S. Patrick, T. Kotiaho, S.A. McLuckey, *Mass Spectrom. Rev.* 13 (1994) 287.
- [53] W.M. David, J. Brodbelt, S.M. Kerwin, P.W. Thomas, *Anal. Chem.* 74 (2002) 2029.